AD 273 562

BOUNDARY FLOW ALONG A CIRCULAR CYLINDER

TECHNICAL REPORT

NO. 204-4

CONTRACT NO. NONR 2119 (02)

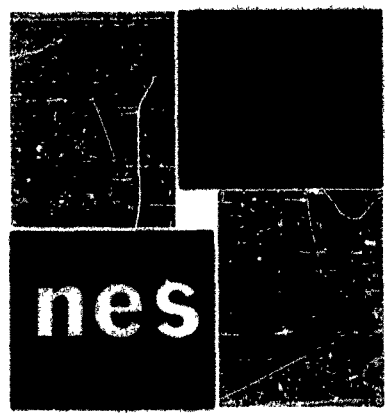

PREPARED FOR

DAVID TAYLOR MODEL BASIN,

BUREAU OF SHIPS, U. S. NAVY

WASHINGTON, D.C.

NATIONAL ENGINEERING SCIENCE CO.

MARCH 1962

BOUNDARY FLOW ALONG A CIRCULAR CYLINDER

Robert O. Reid and Basil W. Wilson

Research conducted through the
Texas A & M Research Foundation (Project 204)
and the National Engineering Science Co. (SN-54 and SN-59)

Projects 204 (Texas A & M) and SN-54, SN-59 (NESCO)
have been supported by the Bureau of Ships
Fundamental Hydromechanics Research Program NS.715-02
administered by the David Taylor Model Basin, U. S. Navy
Contract No. Nonr 2119(02)
and by
The South African Railways and Harbours Administration

Technical Report No. 204-4

NATIONAL ENGINEERING SCIENCE COMPANY
February, 1962

PREFACE

This report represents an improved and extended representation of the results given originally in Section 13 and Appendix B in the first report (No. 204-1) [Wilson, 1960] in this series. Professor R. O. Reid and the undersigned have collaborated in revising the original text and in introducing new material. The results of this study could be of importance in cases of longitudinal flow along long cylindrical objects approximating closely to circular form. They could thus have a bearing on the resistance to motion of submersibles as well as cables in towing operations.

The authors would record their appreciation of the assistance of the following persons: Mrs. Linda Lindsay and Mr. Joe Mitchell for desk and IBM computations respectively (A & M College of Texas); Mr. Guido Zemgals and Mr. Takashi Umehara for drafting (NESCO).

Basil W. Wilson
Consultant

February, 1962
Pasadena, California

CONTENTS

LIST OF FIGURES

LIST OF TABLES

BOUNDARY FLOW ALONG A CIRCULAR CYLINDER

Robert O. Reid[a] and Basil W. Wilson[b]

Abstract

The Karman-Prandtl mixing-length theory for fluid flow over a flat surface with a laminar sublayer near the boundary is adapted to the flow along an infinite circular cylinder on the supposition that flux of momentum inwards towards the boundary is controlled by a continuity condition arising from the radial nature of the convection. Experimental results for smooth and rough pipe flows are invoked to develop the nature of the boundary flow over a range of conditions from the quasi-smooth to the fully turbulent regimes. The drag coefficient for tangential friction is evaluated as a function of Reynolds number and surface roughness. Theoretical indications compare favorably with results from towing tests of stranded cables.

1. Introduction

Longitudinal flow along the outside of a circular cylinder of unlimited length has at least some similarity to pipe flow and flow of a fluid over a flat surface, since the outside surface of a cylinder can be "unwrapped" into a plane of effectively infinite width or topologically turned outside-in to approximate a pipe. Such parallels, though admissible for flow close to the surface, must obviously fail as the distance from the cylinder wall increases. In the following an attempt is made to retain the experimentally known features of the behavior of fluids flowing over a flat surface which accord with Karman-

a Prof. of Phys. Oceanogr., Agricultural and Mechanical College of Texas, College Station, Texas.

b Senior Staff, National Engineering Science Co., Pasadena, California.

Prandtl mixing-length theory, but to impose on the regime a realistic law governing the radial flux of momentum inwards towards the boundary from surrounding concentric layers of fluid.

2. Quasi-Smooth Surface Condition

For quasi-smooth surface conditions, a laminar layer of thickness δ is presumed to exist in contact with the cylinder (Fig. 1a). The longitudinal shear stress τ within this layer is governed by the relationship.

$$\tau = \rho \nu \frac{du}{dy} \; ; \; y \leq \delta \; , \tag{1}$$

in which ρ is the fluid density, ν its kinematic viscosity, u the longitudinal velocity of the fluid (relative to the cylinder) at a distance y from the surface. The latter, in terms of radius r from the center of the cylinder of radius a, is simply

$$y = r - a \; . \tag{2}$$

At the outset it is presumed that the current u and the stress τ are functions of the distance y (or r) only.

Outside of the laminar layer the shear stress is presumed to be governed by the Prandtl-von Karman mixing-length relation for turbulent flow, namely

$$\tau = \rho (ky)^2 \left| \frac{du}{dy} \right| \frac{du}{dy} \; ; \; y \geq \delta \; , \tag{3}$$

where k is the von Karman constant (the value 0.4 being adopted in the calculations which follow).

The inward transport of axially directed momentum through a surface of arbitrary radius r which is concentric with the solid cylinder is $2\pi r \tau$

per unit length of cylinder per unit time. Since it is considered that there is no accumulation of momentum within any finite volume of fluid, it follows that the inward transport of momentum through the surface of radius r must be equal to the transport through any other surface concentric to the latter, including the surface of radius a. At this boundary surface the inward transport of momentum is the same as the axial thrust per unit length exerted by the fluid on the solid cylinder and is equal to $2\pi a\tau_a$, where τ_a is the axial shear stress at $r = a$. Consequently at any arbitrary radius r it follows that

$$\tau = \frac{a}{r}\tau_a = \frac{a}{a+y}\tau_a \quad . \tag{4}$$

Integration of relations (1) and (3), subject to the condition (4) plus the kinematic conditions that u vanish at $y = 0$ and that u be continuous at $y = \delta$, leads to the following expressions for the flow:

$$u = \frac{a\,u_*^2}{\nu}\ln\left(\frac{a+y}{a}\right); \quad y < \delta \tag{5}$$

and

$$u = \frac{a\,u_*^2}{\nu}\ln\left(\frac{a+\delta}{a}\right) + \frac{u_*}{k}\ln\left\{\frac{Q\,(y/a)}{Q\,(\delta/a)}\right\}, \quad y \geq \delta \tag{6}$$

where the function Q in terms of an arbitrary variable α is defined as

$$Q(\alpha) = \frac{\sqrt{1+\alpha} - 1}{\sqrt{1+\alpha} + 1} \tag{7}$$

and the shear velocity u_* is

$$u_* = \sqrt{\frac{\tau_a}{\rho}} \quad . \tag{8}$$

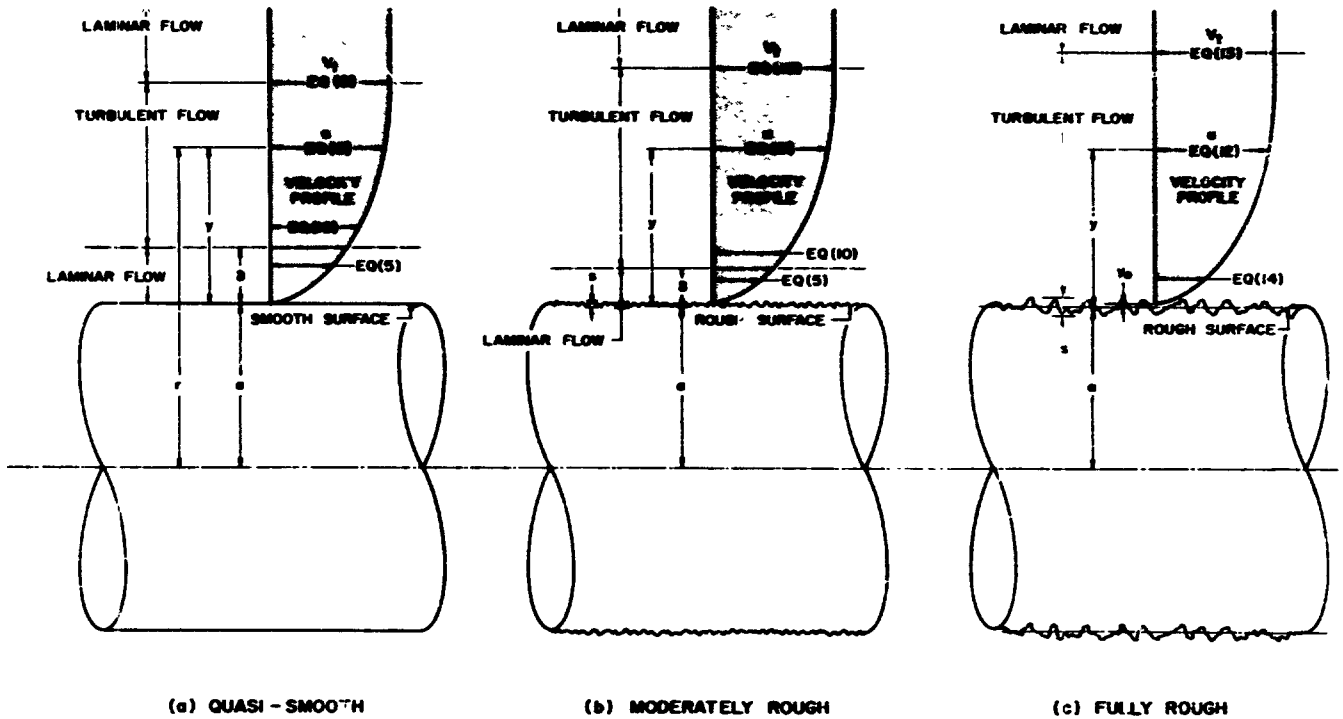

(a) QUASI - SMOOTH (b) MODERATELY ROUGH (c) FULLY ROUGH

FIG. 1: Schematic representations of steady boundary flow along a long circular cylinder with different surface conditions.

Since the function $Q(\alpha) \to 1$ as $\alpha \to \infty^*$, it follows that u approaches the terminal value

$$V_t = \frac{a\, u_*^2}{\nu} \ln\left(\frac{a+\delta}{a}\right) - \frac{u_*}{k} \ln Q(\delta/a) \quad , \tag{9}$$

for $y \gg a$. The quantity V_t represents the speed of the fluid (or axial component thereof) in the region undisturbed by the presence of the cylinder, and is one of the basic independent parameters of the problem (Fig. 1a).

For $\delta < y \ll a$, the general relation (6) for the turbulent region reduces approximately to the form

$$\frac{u}{u_*} = \left(N - \frac{1}{k} \ln N\right) + \frac{1}{k} \ln \frac{u_* y}{\nu} \tag{10}$$

where

$$N = \frac{u_* \delta}{\nu} \quad . \tag{11}$$

Thus the flow near the surface, but above the thin laminar layer, conforms with the classical relation for flow over a flat plate.

3. Fully Rough Surface Condition

For fully rough conditions, the laminar boundary layer is presumed to be non-existent (Fig. 1c), so that (3) alone governs the velocity distribution throughout the fluid. Integration of (3), employing the condition (4)

---

* Note that $Q(\alpha) \to \alpha/4$ and $\ln(1+\alpha) \to \alpha$, as $\alpha \to 0$.

leads to the relation

$$u = \frac{u_*}{k} \ln \frac{Q(y/a)}{Q(y_o/a)} \quad , \tag{12}$$

where y_o is the level at which u vanishes. Presumably the constant of integration y_o depends upon the degree and nature of the surface roughness.

For the case of a fully rough surface, the terminal speed according to (12) has the value

$$V_t = \frac{u_*}{k} \ln \frac{1}{Q(y_o/a)} \tag{13}$$

On the other hand, the velocity distribution near the surface (considering both y_o and $y \ll a$) reduces approximately to the simple log law

$$\frac{u}{u_*} = \frac{1}{k} \ln(y/y_o). \tag{14}$$

Since relations (10) and (14), representing the limiting cases for small y, conform to the formulas applicable to a flat plate, it is tempting to apply the empirical results pertinent to the latter in order to evaluate the parameters N and y_o in terms of measurable quantities.

4. Adaptation of Empirical Relations for Flow over a Flat Plate

The experiments of Nikuradse and others have shown that the velocity distribution in the turbulent region within a pipe and above a flat plate for general conditions of flow (and neutral thermal stability) tends to conform to the relation

$$\frac{u}{u_*} = B + \frac{1}{k} \ln \frac{u_* y}{\nu} \tag{15}$$

where B is a function of $u_* s/\nu$, s being the equivalent sand-roughness diameter of the surface [c.f., Granville, 1958] . For the extreme cases of fully smooth and fully rough surface conditions (for which $u_* s/\nu$ is very small or very large, respectively), the experimental work of Nikuradse indicates that

$$\left.\begin{aligned} &\text{(a)}\ B = 5.5\ , \text{for}\ \phi \ll 1 \\ \text{or}\quad &\text{(b)}\ B = 8.5 - \frac{1}{k}\ln\phi\ , \text{for}\ \phi \gg 1 \end{aligned}\right\} \tag{16}$$

where for convenience we introduce as a symbol of roughness Reynolds Number

$$\phi = \frac{u_* s}{\nu} \ . \tag{17}$$

To secure a generalized formula that will satisfy the extremes represented by (16 a, b) and withal define the velocity distribution for any value of the relative roughness (ϕ), [Sutton , 1953] has proposed a relation for u/u_* which implies that

$$B = 8.5 - \frac{1}{k}\ln\left(\frac{10}{3} + \phi\right) \ . \tag{18}$$

As shown in Fig. 2, the above relation is in close agreement with Colebrook's 1938 empirical relation for the case of "engineering roughness". Also shown in Fig. 2 is the empirical relation of B versus ϕ for Nikuradse sand roughness [Granville, 1958] . To arrive at some compromise between engineering roughness and sand roughness the following relation

$$B = 8.5 - \frac{1}{2k}\ln\left[\left(\frac{10}{3}\right)^2 + \phi^2\right] \tag{19}$$

These are values derived from experiments on pipe flow [cf. Rouse, 1946, pp 194-5] . They become modified very slightly for the case of flow over a flat plate [cf. Schlichting, 1960, p 540] .

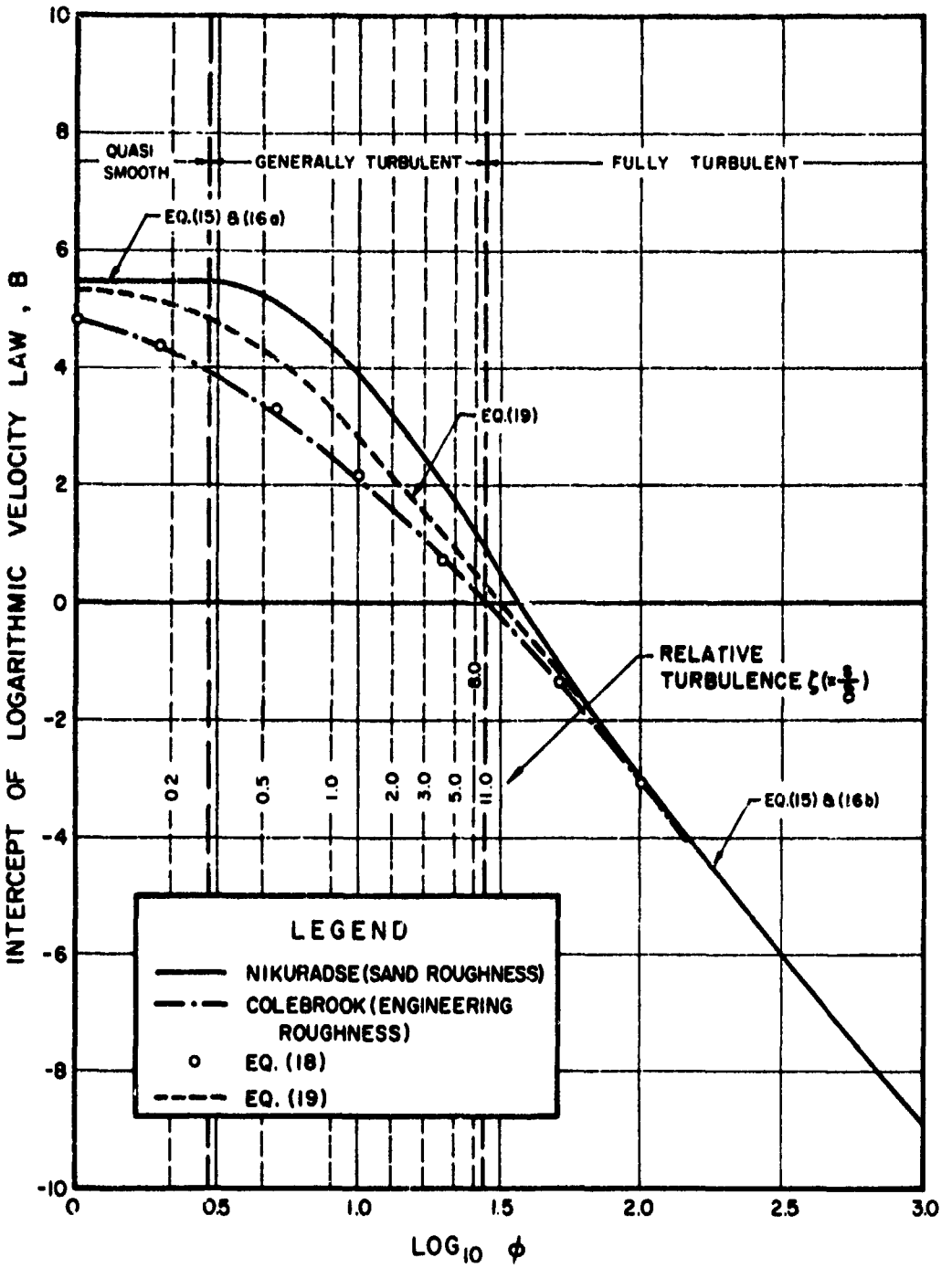

FIG. 2: Dependence of logarithmic velocity-law intercept, B, on roughness Reynolds No., ϕ

is adopted in preference to Sutton's formula. This satisfies the limiting cases (16 a, b) and yields a very satisfactory intermediate transition curve between the fully smooth and fully rough conditions (Fig. 2.). It must be emphasized that either of the suggested relations (18) or (19) is purely a means of summarizing the empirical results in a convenient but approximate manner.

For the fully rough surface condition, relations (15) and (16b) imply that

$$\frac{u}{u_*} = 8.5 + \frac{1}{k} \ln (y/s) \quad , \tag{20}$$

which is of the form (14) provided that y_o is taken as $s/30$. We may anticipate that the fully developed turbulent regime of flow as represented by (14) or (20) occurs at some critical value of the roughness Reynolds number ϕ. For values of ϕ less than this critical number a laminar layer exists, the thickness depending upon the numerical value of N, Eq. (11).

Comparing (10) and (15), it is evident that N is related to ϕ by the relation

$$N - \frac{1}{k} \ln N = B(\phi) \quad , \tag{21}$$

for quasi-smooth conditions of the surface (sub critical value of ϕ). An inspection of (21) reveals that the derivative dN/dB changes sign when

$$N = 1/k = 2.5 \tag{22}$$

which, in terms of B, yields

$$B = \frac{1}{k} (1 + \ln k) = 0.21 \tag{23}$$

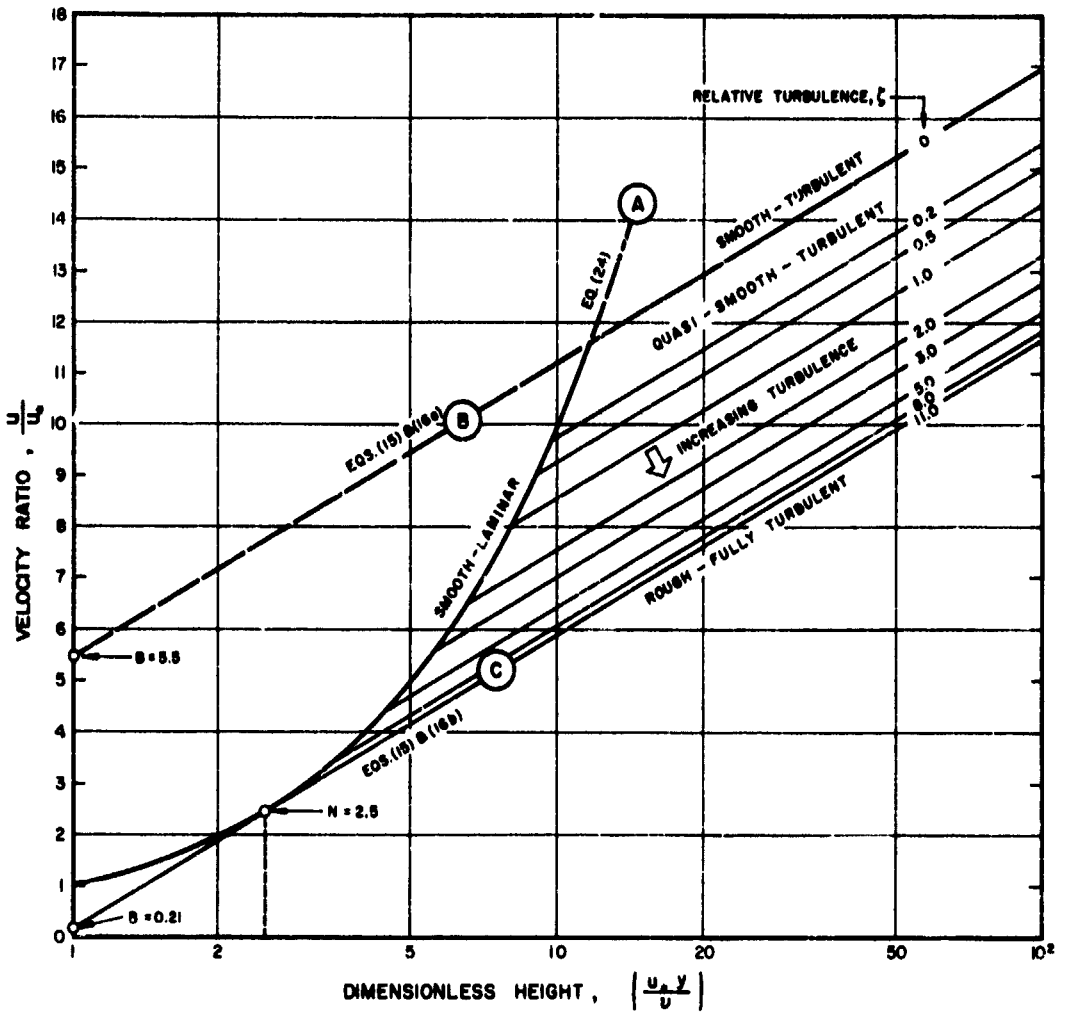

FIG. 3: Dimensionless velocity u/u_*, in the boundary flow as related to dimensionless height, u_*y/ν, above the cylinder surface.

For B greater than 0.21, relation (21) yields two real positive roots for N. In the limiting case for fully smooth surface conditions, B has the maximum value 5.5 for which the corresponding values of N are 0.116 and 11.6 from (21). In the case of the first root, dN/dB is negative. We should expect N to decrease with increasing ϕ, and since B decreases with increasing ϕ, dN/dB should be positive. On this basis the lower root is rejected in favor of the value 11.6.

For values of B less than 0.21, there are no real roots of (21) and consequently the laminar sublayer is undefined, or non-existent. This corresponds to the condition for which the roughness Reynolds number ϕ exceeds the critical value 27.4 according to (19). It is for this super-critical stage that we may expect the fully rough surface condition to prevail.

The implications of this are illustrated in Fig. 3 in which curve (A) defines the purely laminar flow, derived from (5) when $y \leq \delta_l \ll a$, namely

$$\frac{u}{u_*} = \frac{u_* y}{\nu} \tag{24}$$

Curve (B) conforms with relations (15) and (16a) for quasi-smooth conditions of turbulent flow and marks the intercept B = 5.5 on the axis of u/u_*. Curve (C), equivalent to the fully turbulent conditions of (15) and (16b), is parallel to (B) with the slope 1/k, and tangential to (A) at the value $u_* y/\nu = 2.5$ (=N), corresponding to the critical value of ϕ (= 27.4). The intercept of (C) on the u/u_* axis thus defines the minimum value of B in (23), namely 0.21. Below (C) the flow regime is fully turbulent and the laminar layer is non-existent. Between (B) and (C) there is increasing turbulence to lower levels near the cylinder surface, as indicated schematically in Figs. 1.

From (11) and (17) we may define the "relative turbulence" of the flow to be

$$\zeta = s/\delta = \phi/N \tag{25}$$

For the critical value of ϕ (=27.4), the relative turbulence ζ has a value of 11.0, which conveys some idea of the relative magnitudes of the roughness diameter s and the thickness δ of the laminar layer. As this ratio declines to zero so the flow approaches the condition of a quasi-smooth surface regime. Values of relative turbulence are indicated in Fig. 2 and are portrayed by isolines of ζ in Fig. 3, which omits, however, transitional curves between (A) and parallels of (B).

5. Evaluation of Empirico-Theoretical Results

We wish to put the above results in a form whereby it is possible to evaluate the longitudinal drag on the cylinder in terms of the terminal velocity V_t, the radius a and the equivalent roughness s. To this end we introduce two new dimensionless parameters

$$\left.\begin{aligned} &\text{(a)} \qquad R_* = \frac{a u_*}{\nu} \\ &\text{(b)} \qquad R_t = \frac{2a\, V_t}{\nu} \end{aligned}\right\} \tag{26}$$

The first of these is a Reynolds number for the cylinder based upon the surface shear stress via the term u_*; the second is a "radius"-Reynolds Number corresponding to the tangential flow V_t. As a relative measure of surface roughness we use

$$\lambda = s/a \tag{27}$$

which is related to ϕ and R_* by the simple relation

$$\phi = R_* \lambda \ . \tag{28}$$

From the definitions of N, R_*, and R_t it is readily shown that (9) can be rendered in the form

$$R_t = 2R_*^2 \ln (1 + N/R_*) - \frac{2R_*}{k} \ln Q(N/R_*) \tag{29}$$

which applies for $N > 2.5$ ($\phi < 27.4$). Also from (19), (21) and (28) it follows that

$$R_* = \frac{1}{\lambda}\left[N^2 \exp(6.8 - 0.8N) - 11.1\right]^{\frac{1}{2}} \tag{30}$$

for $N > 2.5$. Relations (29) and (30) indicate an implicit relation between R_t and R_* for given value of λ . This relation is readily evaluated numerically by choosing successive values of the parameter N in the range 2.5 to 11.6 for selected values of λ .

If a tangential drag coefficient C_{dt} is now defined such that

$$\tau_a = \frac{1}{2}\rho C_{dt} V_t^2 \ , \tag{31}$$

it then follows from the definitions of u_*, R_* and R_t that

$$C_{dt} = 8 (R_*/R_t) \tag{32}$$

Finally the total axial thrust due to surface drag per unit length of cylinder is given by

$$F_t = C_{dt} \rho \pi a V_t^2 \ . \tag{33}$$

For fully rough conditions of flow along the surface of the cylinder ($\phi > 27.4$) 4) it follows from (13), with $y_o = s/30$, that

$$R_t = -(2R_*/k) \ln Q(\lambda/30) \tag{34}$$

Since λ is generally very much smaller than unity, the above relation simplifies to

$$R_t = \frac{2R_*}{k} \ln \frac{120}{\lambda} \ , \tag{35}$$

for $\phi > 27.4$. From this it follows that

$$C_{dt} = 2 \left[k/\ln (120/\lambda) \right]^2 \tag{36}$$

which is independent of R_t. This limiting value of C_{dt} applies provided that R_t exceeds a critical value which, according to (28) and (35) with $\phi = 27.4$, is given by

$$\left[R_t \right]_c = (137/\lambda) \ln (120/\lambda) \tag{37}$$

For selected values of roughness parameter λ, these limiting values are as follows:

Table I: Reynolds Number for the Threshold of the Fully Rough Regime of Flow

λ	$\left[R_t \right]_c$	C_{dt}
0.001	1,590,000	0.0024
0.010	129,000	0.0036
0.100	9,700	0.0064
1.000	660	0.0140

Equation (36) permits the evaluation of a reasonable upper limit on C_{dt} (for suitably large R_t) by selecting a maximum value of λ. For stranded cable, clearly the radius of the strands cannot exceed the radius of the cable. Accordingly it seems reasonable to consider that λ will be less than unity for most cases. Relation (36) yields $C_{dt} = 0.014$ for $\lambda = 1$ as a reasonable upper limit, provided that R_t exceeds 660.

The minimum value of C_{dt} for given R_t corresponds to the fully smooth condition for which $N = 11.6$ and $B = 5.5$. Using (9), (11), (26) and (32) it can be shown, for large R_t ($> 10^4$), that the drag coefficient

for smooth conditions is given implicitly by

$$\left.\begin{aligned} &\text{(i)} \quad C_{dt} = 2/\beta^2 \\ &\text{(ii)} \quad R_t = (\beta/2)\, e^{k(\beta - 5.5)} \end{aligned}\right\} \tag{38}$$

where β serves purpose as a correlating parameter. Even for R_t as large as 10^8 this yields minimum values of C_{dt} exceeding 0.001. More generally than (38), the lower limit of C_{dt} as a function of R_t, for a smooth cylinder ($\zeta = 0$), is given by relations (29) and (32) for the specific value $N = 11.6$.

The properties of the fluid drag along the circular cylinder may now be examined by determining corresponding values of C_{dt} and R_t for the transitional condition from relations (29), (30), and (32) for different values of the roughness parameter λ. The terminal values of C_{dt} for a particular λ must agree with (36) for R_t exceeding the critical value defined by (37). The envelope (lower-limit) curve must conform to (38) for values of R_t exceeding, say, 10^3. The resulting family of relationships is shown in Fig. 4. These results, which in effect utilize the considerable experimental evidence on wall friction accumulated from flow in pipes and over flat surfaces, may be expected to provide reasonably precise guidelines of behavior in respect to the circumferential longitudinal drag on a circular cylinder of given roughness and indefinite length.

To complete the information condensed in Fig. 4, isolines of relative turbulence ζ have been included to shed light on the nature of the laminar sub-layer, when extant. These isolines, as might be expected, parallel the lower-limit envelope curve for a smooth cylinder ($\zeta = 0$) and occupy the region of the diagram where the isolines of roughness parameter λ are transitional between the envelope curve and their values of constant C_{dt}.

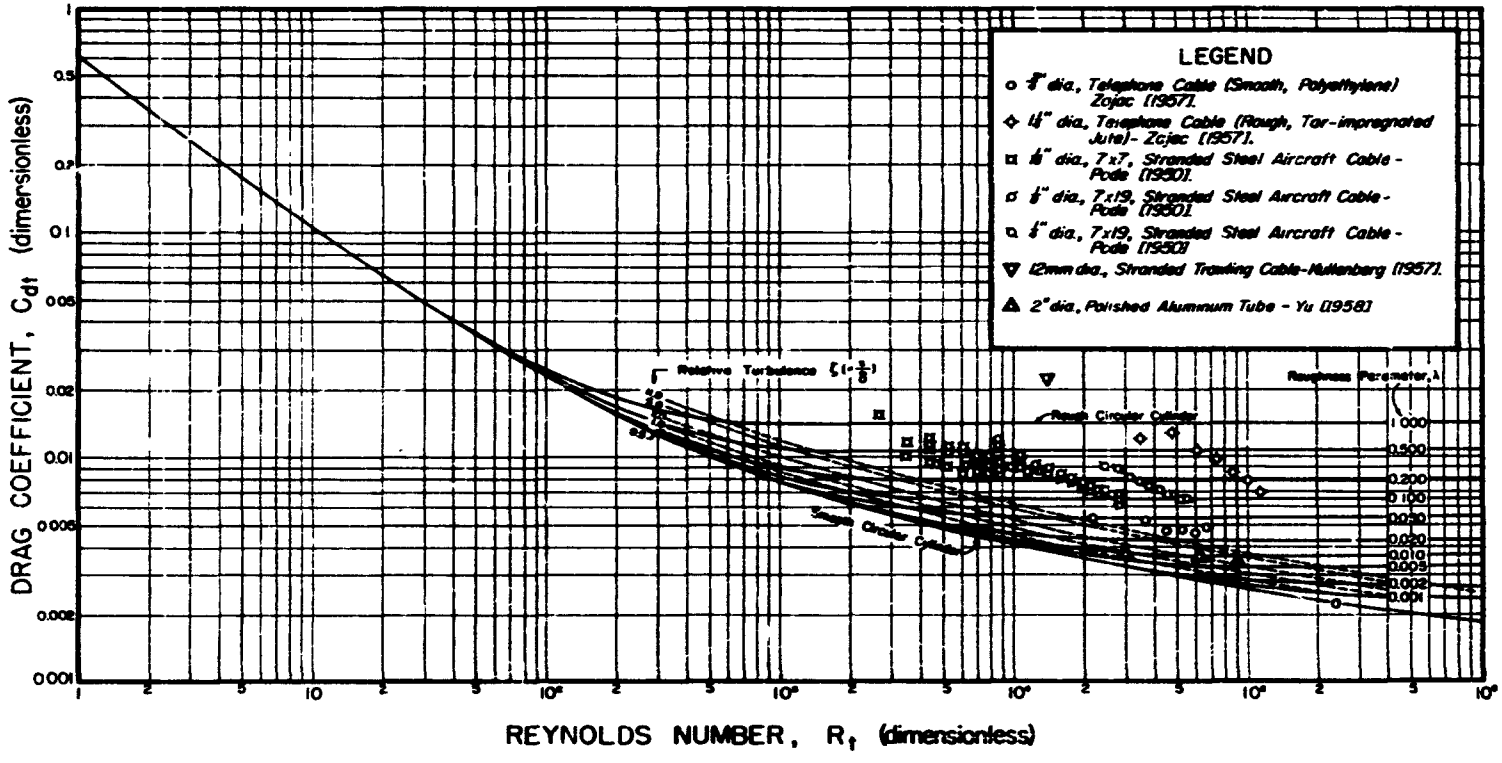

FIG. 4: Relationship of tangential drag coefficient, C_{dt}, to 'radius' Reynolds No., R_t, for different degrees of cylinder roughness, .

6. Experimental Confirmation of the Theory

Available experimental information on the nature of tangential drag along a long circular cylinder of varying degrees of roughness seems to be rather sparse. The major source of data would appear to be the experiments conducted at the David Taylor Model Basin, U. S. Navy, by towing stranded cables in water [Pode, 1950; Zajac, 1957] . From measurements of the angles of inclination of the cables to the trajectories of the tow-points, these experiments showed that the normal drag, F_n , at right angles to the cables, complied with the so-called "sine-square" law, namely

$$F_n = \frac{1}{2} C_{dn} \rho(2a) V_n^2 , \tag{39}$$

in which C_{dn} is the normal drag coefficient and V_n the normal component of the velocity, V, of the flow round the cable. When the latter is inclined to the flow at an angle ψ ,

$$V_n = V \sin \psi . \tag{40}$$

For the same inclination, the tangential flow along these cables would have been

$$V_t = V \cos \psi \tag{41}$$

and since the integrated F_t of Eq. (33) was measured at the towing carriage, both C_{dt} and R_t are calculable in terms of Eqs. (33) and (26) respectively from the quoted results of the experiments. Reduction of Pode's and Zajac's data in this manner thus serves to establish the series of plotted points in Fig. 4.

These experimental data are clearly of the same order of magnitude as the indicated theoretical trends. There is, however, an obvious disposition of groups of points favoring some secondary dependence of C_{dt} upon R_t. Before discussing this, it seems appropriate to take the centroids of groups of like-plotted points as an indication of average C_{dt}

and R_t correspondence and hence read from the theoretical curves the expected degree of roughness λ of the cables. The results are recorded in Table II, in which for comparison are such values of λ as can reasonably be assessed from cross-sectional diagrams of equivalent stranded wire cables. While the information of column (6) is insufficiently exact to permit a satisfying comparison, it would appear to indicate that the depth of crevices between strands in stranded wire cables is probably an effective relative measure of roughness.

Table II: Apparent Roughness Parameters of Cables

(1)	(2)	(3)	(4)	(5)	(6)
Cable diameter 2a (ins)	Type and covering	Mean Drag Coefficient C_{dt}	Reynolds No. R_t	Theor. Roughness Parameter λ	Measured Roughness Parameter λ
1/16	7 x 7	0.0096	6.2×10^3	0.35	0.36
1/8	7 x 19	0.0080	1.75×10^4	0.22	0.34
1/4	7 x 19	0.0073	3.9×10^4	0.16	0.34
3/4	Telephone; Polyethylene	0.0050	4.0×10^4	0.04	0.10(?)
1 1/4	Telephone; Tar-impregnated jute	0.0096	7.1×10^4	0.38	(?)

The secondary dependency of C_{dt} upon R_t now calls for comment. Pode [1950] reported the fact that stranded cable has a natural tendency in towing tests to yaw laterally out of the vertical plane of the tow point. The reason for this is attributed to the non-symmetrical cross-section which the cable presents to the flow. Owing to the lay of the strands and the general inclination of the towed cable there is a tendency towards tangential flow down the strands on one side of the cable and normal flow across the strands on the

opposite side. The reaction from this provides the unbalance contributing to the yaw and the accompanying slight uplift of the towed cable. If the speed of tow be small, the angle ψ of cable inclination will be quite large, resulting in almost completely transverse drag across individual strands and wires as shown in Fig. 5(a). On the other hand if the speed of tow be great, the angle ψ becomes small and the tendency is towards the unbalance noted above (Fig. 5(b)). It is suggestive from this that the relative roughness λ of the cable at low towing speeds will be greater than at high speeds because of the partially smoother flow down the strands at small angles of cable inclination. It would appear logical to expect therefore that C_{dt} values at lower Reynolds numbers will be greater than those at higher Reynolds numbers, in keeping with the systematic trends revealed by Pode's and Zajac's data in Fig. 4.

It is outside the province of the present paper to attempt to analyze the influence of the cable stranding in more detail than this, but it seems noteworthy in passing that the secondary dependency of C_{dt} upon R_t for stranded cable appears to conform to a relationship of the Blasius type, namely

$$C_{dt} = \frac{K}{[R_t]^2} \tag{42}$$

in which K is a constant which could be expected to depend on the cable diameter.

Another source of experimental information lies in the work of Yu [1958] who measured the surface shearing stress on a 2-inch diameter polished aluminum cylinder 12 ft. long, deriving from longitudinal flow of air in a wind tunnel parallel to the cylinder axis. Taking only his observations made at 8 ft from the nose of the cylinder to escape the entry effect, these yield the following data:

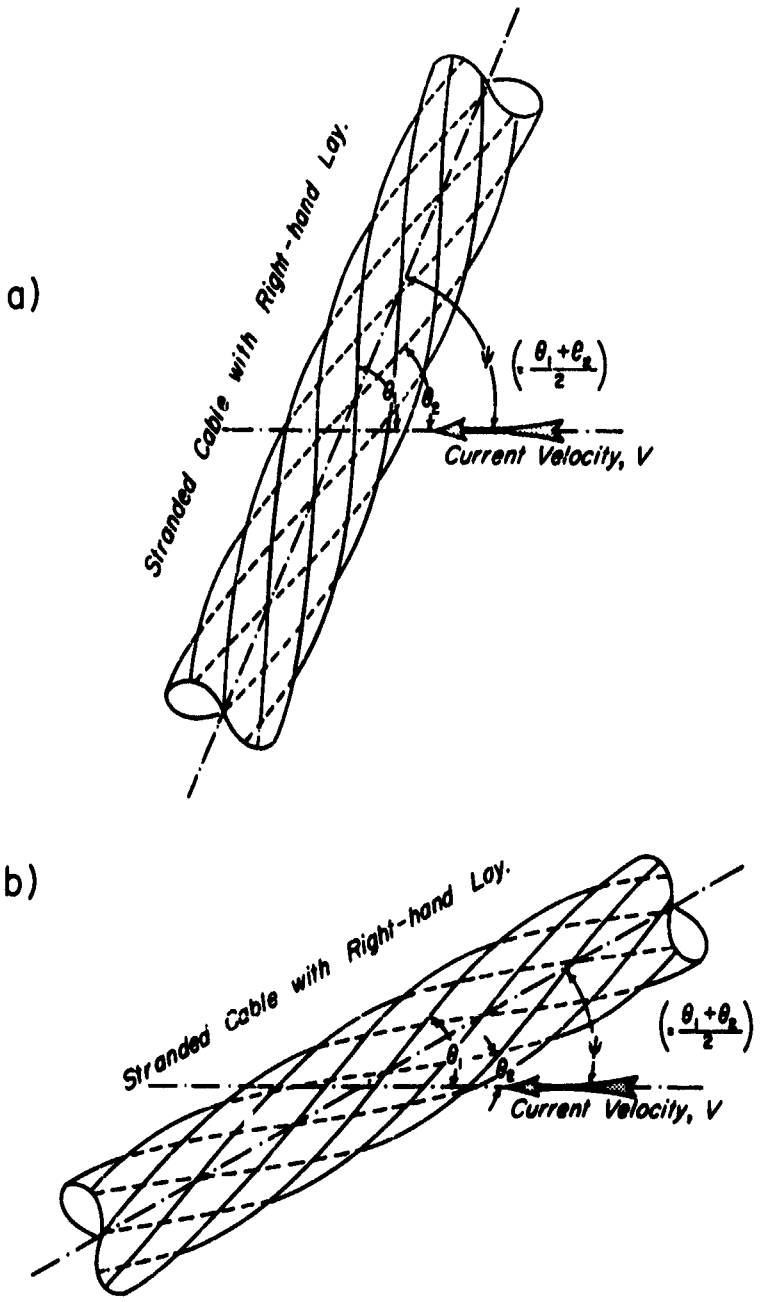

FIG. 5: Schematic diagram of fluid flow round a stranded cable at (a) low towing speed (b) high towing speed.

Table III: Flow along a Smooth Cylinder; Results of Yu [1958]

(1)	(2)	(3)	(4)	(5)	(6)
Stream Velocity V_t (ft/sec)	Reynolds No. R_t	Measured Shear Velocity u_* (ft/sec)	Derived Drag Coefft. C_{dt}	Apparent Roughness Parameter λ (from Fig.4)	Relative Turbulence ζ (from Fig.4)
30	3.05×10^4	1.30	0.0037	0.010	0.8
60	6.15×10^4	2.58	0.0036	0.010	2.0
90	9.01×10^4	3.64	0.0034	0.008	2.2

The values of λ and ζ given in columns (5) and (6) of Table III are derived from Fig. 4 where the data of columns (2) and (4) are seen to plot in good harmony with the theoretical curves. The inference is that the sand roughness diameter, s, of the "smooth"cylinder was of the order of 1/100 inch. The height of the laminar sub-layer at the three stream velocities (30, 60 and 90 ft/sec) is indicated by the quotient λ/ζ and approximates 1/80, 1/200, and 1/300 inch respectively.

7. Conclusions

The results of this analysis suggest that the tangential drag coefficient C_{dt}, as defined by Eq. (31), for flow along a circular cylinder, may be expected to lie within the limits 0.002 and 0.02, depending on roughness, within a practical working range of radius-Reynolds Numbers R_t, considered to be greater than 10^3. Experimental results for towed stranded cables indicate conformance to the indicated theoretical trends when the velocity of flow along the cable is taken as the tangential component along the cable of the velocity of actual flow, which may be oblique to the

cable. The depth of crevices between major strands of the cables, in relation to the cable radius, would appear to be a reasonable measure of the roughness parameter dictating the magnitude of the drag coefficient in any given case. In stranded cables the value of C_{dt} would appear to be additionally dependent on the angle of obliquity of the cable to the flow, in consequence of the lay of the strands. Experimental results for a smooth cylinder are in good agreement with the theory; it is, in fact, encouraging and noteworthy that none of the empirical data for C_{dt} fall below the lower-limit curve for smooth flow for any value of R_t in Fig. 4.

8. Acknowledgement

Publication of this paper is made possible through the courtesy of the David Taylor Model Basin, U. S. Navy, under whose sponsorship this work has been undertaken as part of a study (Contract Nonr 2119(02) on the dynamics of deep-sea mooring cables. The authors would record their appreciation of this support.